NEW SCHEME TO GENERATE A MULTI-TERAWATT AND ATTOSECOND X-RAY PULSE IN XFELS

T. Tanaka*
RIKEN SPring-8 Center, Koto 1-1-1, Sayo, Hyogo 679-5148, Japan

Abstract

A new scheme to upgrade the source performance of X-ray free electron lasers (XFELs) is proposed, which effectively compresses the radiation pulse, i.e., shortens the pulse width and enhances the peak power of radiation, by inducing a periodic current enhancement with a long-wavelength laser and applying a temporal shift between the X-ray and electron beams. Calculations show that a 10-keV X-ray pulse with the peak power of 6.6 TW and pulse width of 50 asec can be generated by applying this scheme to the SACLA XFEL facility.

INTRODUCTION

In order to investigate unknown phenomena with a photon beam, its size should be as small as possible both in space and time: its focal size should be ideally smaller than the typical dimension of the target, and its pulse width should be shorter than the typical time scale for the target to change. It should be noted, however, that the focal size and pulse width can never be smaller than the wavelength because of the uncertainty of light. This puts a lower limit on the focal size and pulse width of any kind of lasers.

In the long-wavelength region such as the optical and infrared regions, a focal size and pulse width that are close to these theoretical minima have been already achieved with the state-of-the-art laser technologies. In other words, optical lasers with the focal size less than 1 μm and the pulse width of around several femtoseconds are readily available. On the other hand, the situation is completely different in XFELs having wavelengths four orders of magnitude shorter than the optical lasers: the attainable focal size and pulse width are 50 nm and several femtoseconds, respectively, being far from the theoretical minima, i.e., 0.1 nm and several hundreds of zeptoseconds. It is worth noting that the focal size has been reduced step by step by means of improving the x-ray optics, and possibly will go down to several nm in the near future. On the other hand, there have been no means to compress the XFEL pulse corresponding to the laser pulse compression scheme in the long-wavelength regions. Instead, a number of proposals have been made [1]-[6] to shorten the pulse width at the expense of the reduction of the effective charge contributing to lasing, in which shorting the pulse width does not necessarily mean the enhancement of the peak laser power.

In order to deal with the issue, a novel scheme has been recently proposed [7], in which the XFEL pulse is effectively compressed: the pulse width is shortened and the laser peak power is enhanced as well. In this paper, the principle of the new scheme is introduced and several calculation results to quantify the laser performance are presented.

* ztanaka@spring8.or.jp

PRINCIPLE OF OPERATION

The principle of operation is first explained. Figure 1 shows the schematic diagram of the accelerator layout to apply the proposed pulse compression scheme.

In addition to ordinary components for XFELs, two extra elements are installed before the undulator section, which generates an electron beam having a special bunch structure to realize the bunch compression scheme.

The first one is the slotted foil that has been originally proposed for shortening the XFEL pulse [1] and demonstrated in LCLS. The metal foil installed int the bunch compressor (BC) scatters the electrons and spoils the beam emittance, and thus suppresses the lasing region in the bunch. Because of the strong correlation between the longitudinal coordinate s and horizontal coordinate x at the BC section, lasing is suppressed in the corresponding head and tail of the bunch and thus the XFEL pulse width can be controlled. Note that its function in our scheme is to set a defined temporal window of lasing and define the lasing domain in the electron bunch.

The second one is the E-SASE (enhanced SASE) section in which an optical laser (E-SASE laser) with a wavelength of λ_E is injected synchronously with the electron bunch to a long-period undulator whose fundamental wavelength equals λ_E. In the following dispersive section, the energy modulation is converted to the density modulation with the pitch of λ_E and thus a comb-like current distribution is created in the electron bunch.

After the two processes described above, the current distribution is give as

$$I(s) = [I_u(s) + I_o(s)]E(s),$$

where $I_u(s)$ and $I_o(s)$ denote the current distributions just after the BC section. The former refers to the electrons that are scattered by the foil and do not contribute to lasing and the latter to the electrons that are scattered and do not contribute to lasing. The horizontal beam size at the BC section depends on the energy chirp for the bunch compression and other intrinsic factors such as the beam emittance, betatron function and energy spread. If the latter effect is negligible compared to the former one, $I_o(s)$ is expected to have a rectangular profile. In reality, there exists a fringe region at the boundary between $I_o(s)$ and $I_u(s)$ because of

ISBN 978-3-95450-126-7

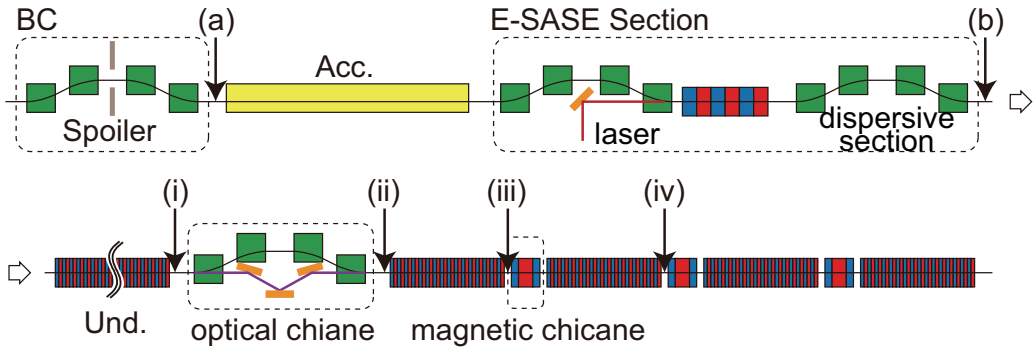

Figure 1: Accelerator layout to realize the proposed pulse compression scheme.

the intrinsic factors. Approximating the beam profile determined by these intrinsic factors a Gaussian profile with the standard deviation of σ_f, $I_o(s)$ is given by

$$I_o(s) = \frac{1}{\sqrt{2\pi}\sigma_f}\int_{s_1}^{s_2} I(s')\exp\left[-\frac{(s-s')^2}{2\sigma_f^2}\right]ds',$$

$$I_u(s) = I(s) - I_o(s),$$

where s_1 and s_2 are the longitudinal coordinate correlating to the horizontal coordinate defining the aperture of the slot, and $I_(s)$ is the original current distribution without the effect of the foil insertion.

The function $E(s)$ is a periodic function with the period of λ_E and denotes the current enhancement by the E-SASE scheme. If R_{56} at the dispersive section is appropriately set, it is given by [3]

$$E(s) = \sum_j \frac{eB}{1+B^{1/e}}\frac{1}{1+16B^2[(s/\lambda_E)-(\theta/2\pi)-j]^2},$$

where $B = \Delta\gamma/\sigma_\gamma$ and $\Delta\gamma$ is the amplitude of the energy modulation induced by the E-SASE laser, σ_γ is the r.m.s. energy spread and e denotes the base of the natural logarithm. The phase parameter θ refers to the timing jitter between the electron bunch and E-SASE laser pulse, and fluctuate between $-\pi$ and π shot by shot.

Using the above equations, current distributions after the respective sections have been calculated for the electron bunch with the peak current of 3.5 kA and the r.m.s. bunch length of 40 fsec. Figure 2(a) shows the current distribution just after the BC section. The foil slot has been assumed to have the horizontal aperture corresponding to $s_1 = -4.4$ μm and $s_2 = 3.6$ μm, and σ_f has been assumed to be 0.2μm. Compared to the original Gaussian function, the lasing domain (black line) is definitely confined. It should be noted, however, that there exists a fringe region defined by σ_f. If σ_f is too long, the boundary of the lasing domain is not clearly defined and thus the effect of the slotted foil is lost, which leads to a poorer contrast of the main pulse [7]. It is thus important to shorten σ_f as much as possible for the proposed scheme to work.

Figure 2(b) shows the current distributions after the E-SASE section, in which $\lambda_E = 800$ nm,$B = 5$ and $\theta = 0$ have been assumed. A comb-like current distribution with the pitch of 800 nm is found, and each current peaks are enhanced by a factor of nearly 5, being equal to the parameter B. The E-SASE laser power to achieve $B = 5$ is estimated to be around 1 GW fop a 10-period undulator. If we assume relatively a long pulse of 1 psec, the peak power of 1 GW corresponds to the laser pulse of 1 mJ, which is easily available with the state-of-the-art laser technology. The reason why we assume a long pulse (much longer than the bunch length) is to relax the requirement on the timing synchronization between the E-SASE laser and electron bunch.

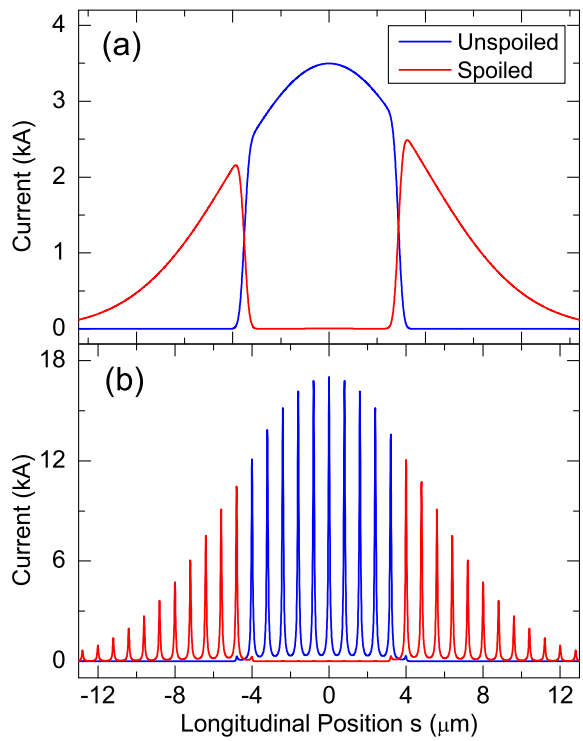

Figure 2: Calculated current distributions after (a) the bunch compressor with the slotted foil and (b) ESASE sections.

Now let us explain the procedure of how to create a solitary pulse from the comb-like current distribution and how to amplify it, using Fig. 3. Also refer to Fig. 1 for the index numbers to indicate the amplification process.

ISBN 978-3-95450-126-7

In the process (i), X-ray pulse train with an interval of λ_E is created by the normal SASE process, which reflects the temporal profile of the electron bunch having the comb-like current distribution. The undulator length in this process should not be too long to damage the electron bunch through the SASE process.

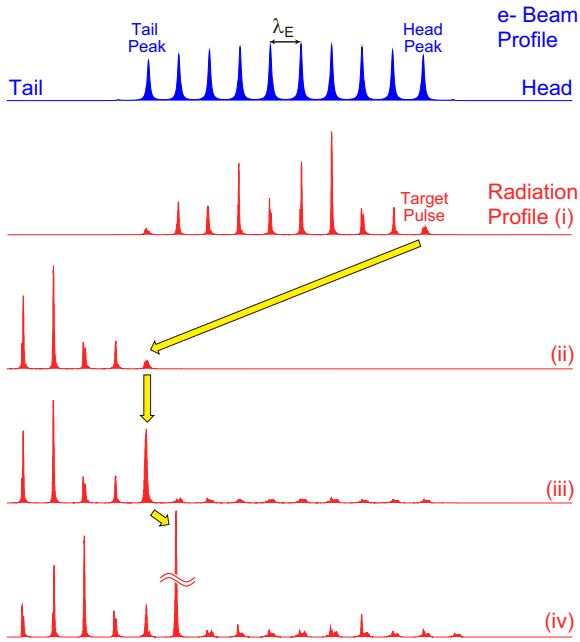

Figure 3: X-ray pulse growth in the early stage of FEL amplification.

In the process (ii), the electron bunch is separated from the X-ray. Then instead of the monochromator as in the case of self-seeding scheme, an optical chicane composed of a number of reflecting mirrors is inserted to give a temporal delay to the X-ray. This delay should be slightly larger than that of the delay for the electron bunch so that the X-ray pulse train is shifted backward with respect to the electron bunch. To be specific, the backward shift distance should be equal to $(N_{pk} - 1)\lambda_E$, where N_{pk} is the number of current peaks contained in the lasing domain of the electron bunch. This is a condition to synchronize the leading X-ray pulse in the train (target pulse) with the current peak located at the tail end of the lasing domain (tail peak).

In the process (iii), the electron bunch and X-ray are injected to the next undulator. Because the microbunch created in the process (i) is washed out when the electron bunch passes through the magnetic chicane, we need a sufficiently long undulator so that the SASE process starts again at the current peak positions except for the tail peak position, where the target pulse works as the seeding light and amplification is launched immediately. In addition, other X-ray pulses are not positioned in the lasing domain and thus are not amplified. It is thus possible to selectively amplify the the target pulse, by adjusting the undulator length adequately.

In the process (iv) where the target pulse is sufficiently amplified at the tail peak, the electron bunch is delayed by the magnetic chicane, and the X-ray pulse train is shifted forward by the distance of λ_E. Then, the target pulse is positioned at the current peak just ahead of the tail peak, where the electron beam quality is not yet degraded (i.e., the energy spread is not yet increased) and is still "fresh". The amplification of the target pulse thus continues.

It should be noted that the X-ray pulse just behind the target pulse also arrives at the position of the current peak (tail peak) and can be amplified. The amplification gain is, however, much lower than that of the target pulse, because the beam quality at the tail peak is significantly degraded during the amplification process of the target pulse. The bottom line in the process (iv) is that only the target pulse is selectively amplified as in the process (iii).

The above process (iv) is repeated until the target pulse arrives at the leading current peak in the lasing domain (head peak). Then the peak power of the target pulse is significantly amplified. If there are still more undulator segments available, the amplification of the target pulse can be continued by shifting it backward to the position of the tail peak.

EXAMPLE

In order to evaluate the expected laser performance by applying the above scheme, FEL simulations have been performed for the electron bunch having the current distribution shown in Fig. 2(b), under an assumption that an 8-GeV electron bunch with the normalized emittance of 0.7 μm and the uncorrelated energy spread of 10^{-4} is injected to undulators with the K value of 2.18 and magnetic period of 18 mm. Note that the photon energy is 10 keV, the ordinary SASE saturation power is around 20 GW, and the pulse width is around 20 fsec.

The undulator layout including the magnetic and optical chicane is schematically illustrated in Fig. 4. Each undulator segment is 5 m long and the drift section in between is 1.15 m long. Two optical chicanes are inserted and the total number of undulator segments is 24. They are determined to be consistent with the dimension of the SACLA undulator hall.

The first 4 segments correspond to the process (i), and the following optical chicane to the process (ii). After the chicane, the target pulse is selectively amplified at two undulator segments. Then the electron bunch is delayed and the target pulse is shifted forward and amplification continues. After the 15th segment where the target pulse arrives at the head peak, it is shifted backward to the tail peak again.

All the calculations have been performed with the FEL simulation code SIMPLEX[8]. Note that the energy spread at the current peak position is increased by the energy modulation induced in the E-SASE process, which are also taken into account in the simulations.

The X-ray temporal profiles at the exits of the 4th, 7th, 10th and 24th (final) segments, retrieved from the simulation results are shown in Fig. 5. At the exist of the 4th seg-

ISBN 978-3-95450-126-7

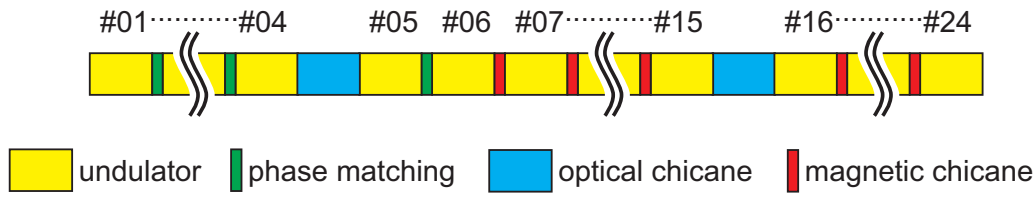

Figure 4: Layout of the undulator, optical- and electron-delay chicanes assumed in the calculation.

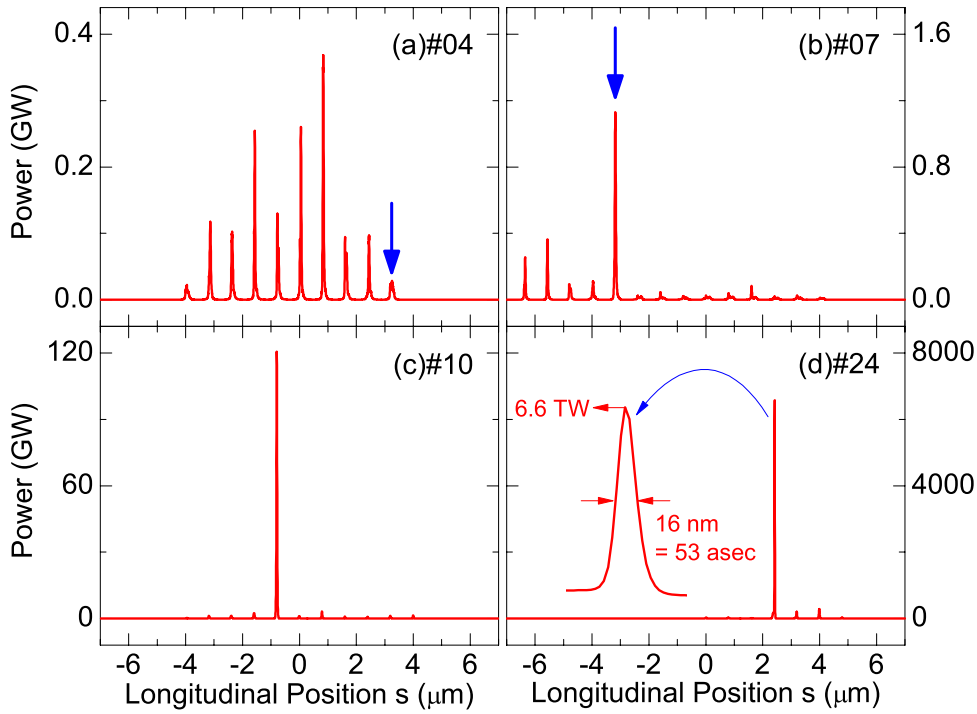

Figure 5: X-ray pulse temporal structures calculated at the ends of different undulator segments.

ment, an X-ray pulse train is found that reflects the comb-like current distribution. Among the pulses, the target pulse indicated by an arrow is selectively amplified in the following undulator segments. As a results, nearly a solitary pulse is generated at the exit of the 10th segment. Until this segment, the target pulse is amplified exponentially and reaches nearly 100 GW, being close to the saturation power for the 17 kA current peak. In the ordinary SASE process, it is not possible to increase the peak power beyond this level. In the proposed scheme, however, the target pulse can be continuously amplified by the fresh peak, which leads to a drastic enhancement of the peak power. As a result, an X-ray pulse with the peak power of 6.6 TW and pulse width of 53 asec is generated at exist of the final segment. Compared to 20 GW and 20 fsec to be obtained in the ordinary SASE process, the XFEL pulse is compressed by a factor of 300.

Now let us look to the evolution of the XFEL pulse segment by segment. Figure 6 shows the pulse width and peak power of the target pulse calculated as a function of the segment number after the formation of the solitary pulse (7th segment).

We find that after creation of the solitary pulse, its peak power P increases not exponentially but quadratically as the segment number, i.e., $P \propto z^2$, where z is the undulator length measured from a certain reference position, as shown in the dashed red line. On the other hand, the pulse width σ_z decreases as the segment number according to $\sigma_z \propto z^{-1/2}$ as shown in the dashed blue line. These dependences on the undulator length are similar to what are found in the superradiant FEL regime.

TOWARD REALIZATION

In order to implement the proposed pulse compression scheme in XFEL facilities, various R&Ds are required. For example, the magnetic chicane, which are installed at almost every drift section, should be as compact as possible. Thus the utilization of permanent magnets instead of electromagnets should be explored. In addition, the beam parameters should be optimized for the slotted foil and E-SASE schemes to work properly. What is more interesting and important is to consider a scheme to eliminate the satellite pulse, which is seen in Fig. 5(d).

ISBN 978-3-95450-126-7

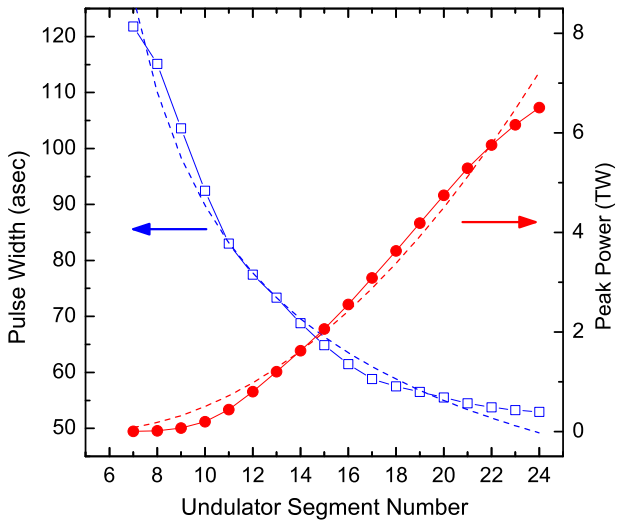

Figure 6: Pulse width (blue) and peak power (red) as a function of the segment number. The dashed lines show the typical curve for the superradiant FEL regime.

REFERENCES

[1] P. Emma, K. Bane, M. Cornacchia, Z. Huang, H. Schlarb, G. Stupakov, and D. Walz, Phys. Rev. Lett. 92, 074801 (2004).

[2] P. Emma, Z. Huang, and M. Borland, in Proceedings of FEL 2004 (Trieste, Italy, 2004), p. 333.

[3] A. A. Zholents, Phys. Rev. ST Accel. Beams 8, 040701 (2005).

[4] E. L. Saldin, E. A. Schneidmiller, and M.V. Yurkov, Phys. Rev. ST Accel. Beams 9, 050702 (2006).

[5] W. M. Fawley, Nucl. Instrum. Methods Phys. Res., Sect. A 593, 111 (2008).

[6] Y. Ding, Z. Huang, D. Ratner, P. Bucksbaum, H. Merdji, Phys. Rev. ST Accel. Beams 12, 060703 (2009).

[7] T. Tanaka, Phys. Rev. Lett. 110, 084801 (2013)

[8] T. Tanaka, in Proceedings of FEL 2004 (Trieste, Italy, 2004), p. 435.

ISBN 978-3-95450-126-7